



Full Length Article

New Fricke Xylenol Liquid detector doped with methylene blue (FXL-mblue) irradiated with red LED light

Lucas Nonato de Oliveira^{a,b,*}, Eriberto Oliveira do Nascimento^a, Linda V.E. Caldas^b

^a Instituto Federal de Educação, Ciência e Tecnologia de Goiás - IFG, Campus Goiânia, Rua 75, n 46, Goiânia, GO, 74055-110, Brazil

^b Instituto de Pesquisas Energéticas e Nucleares, Comissão Nacional de Energia Nuclear-IPEN/CNEN, Av. Prof. Lineu Prestes, 2242, 05508-000, São Paulo, SP, Brazil



ARTICLE INFO

Keywords:

New fricke detector
UV-Vis technique
Red LED source Light

ABSTRACT

In photodynamic therapy, a beam of incident light on the target causes interactions with the photosensitizing agent in the patient, subsequently killing cancerous cells through chemical and biological processes. The objective of this work was to describe for the first time the use of the FXL-mblue detector in dosimetric applications with irradiations from red LED light and using the UV-Vis spectrophotometry as an evaluation technique. The FXL-mblue samples were irradiated with doses of 2.40 kJ/cm² up to 21.6 kJ/cm² using a red LED light system. The results showed good results on uncertainties, sensitivity, reproducibility, repeatability, minimum detectable dose (MDD) and fading times for a promising dosimeter in measurements with visible light. In conclusion, the results indicate good dosimetric characteristics which could be used in quality control of photodynamic therapy measurements.

1. Introduction

Chemical dosimeters have been used in measurements of radiotherapy [1], diagnostic radiology [2,3], and nuclear medicine [4]. Historically, one of these initially viable dosimeters is the so-called Fricke dosimeter, which has ferrous sulfate and sulfuric acid in its solution, and was used for high doses [5]. Twenty years ago, the original solution of the Fricke was modified by adding two-component reagents as xylenol orange and gelatin from pig skin, forming the Fricke Xylenol Gel (FXG) dosimeter [6]. FXG works basically by converting ions from Fe⁺² to Fe⁺³ due to the incident radiation; the ions are directly proportional to the dose absorbed by the dosimeter [7]. In this phase, the dosimeters in gels could be applied in 3D dosimetry, occupying the space of a simulator object of some part of the human body and irradiated providing important information for the treatment of the patient before and after irradiation [8,9].

In the next phase, several changes in the Fricke dosimetry were made, either in the concentrations of its reagents, such as xylenol orange, sulfuric acid, water, nanoparticles, among other reagents [10–14] to improve its sensitivity [15], control fading for future evaluations, or even other alternatives in terms of dosimetric gels applied in energy bundles and absorbed doses compatible with linear accelerators [16,17].

The question of the irradiation energy can define which injury to

treat and how deep the rays must reach and annihilate cancer cells, thus not only high energy measurements are carried out with chemical dosimeters. Some studies have shown dosimeters with effectiveness of UVA dose measurements [18,19], and it is possible to obtain important dosimetric information from these researches as stability and sensibility measurements.

The combination of light from light-emitting diodes (LEDs) and a dosimeter that is capable of detecting and/or exchanging its characteristics due to incidence of that light, could bring useful results to the scientific community regarding the improvement in treatments of photodynamic therapy (PDT) [20,21].

It is exactly in this context that this work concentrates, as an alternative for quality control program on a new detector Fricke Xylenol Liquid doped with blue methylene (FXL-mblue). In this work an irradiation system was built in which the source is a red LED lamp, connected to an electrical system and to the Raspberry Pi computer controller. The objective of this work was to describe for the first time the use of the FXL-mblue detector in dosimetric applications with irradiations from red LED light and using the UV-Vis spectrophotometry as an evaluation technique.

* Corresponding author. Instituto Federal de Educação, Ciência e Tecnologia de Goiás - IFG, Rua 75, n0 46, Campus Goiânia, 74055-110, Goiânia, GO, Brazil.
E-mail address: lucas@ifg.edu.br (L. Nonato de Oliveira).

Table 1
Chemical characteristics of the reagents that form the FXL-mblue solution.

Reagent	Molecular formula	Molecular weight (g/mol)	Concentration (mM)	Manufacturer
Xylenol orange	$C_{31}H_{28}N_2O_{13}SNa_4$	760.58	0.1	Exodo/Brazil
Ferrous ammonium sulfate	$Fe(NH_4)_2(SO_4)_2 \cdot 7H_2O$	278.01	0.7	Dinâmica/Brazil
Sulfuric acid	H_2SO_4	98.08	25	Exodo/Brazil
Methylene blue	$C_{16}H_{18}ClN_3S \cdot H_2O$	319.85	$0.6 \cdot 10^{-3}$	Neon/Brazil

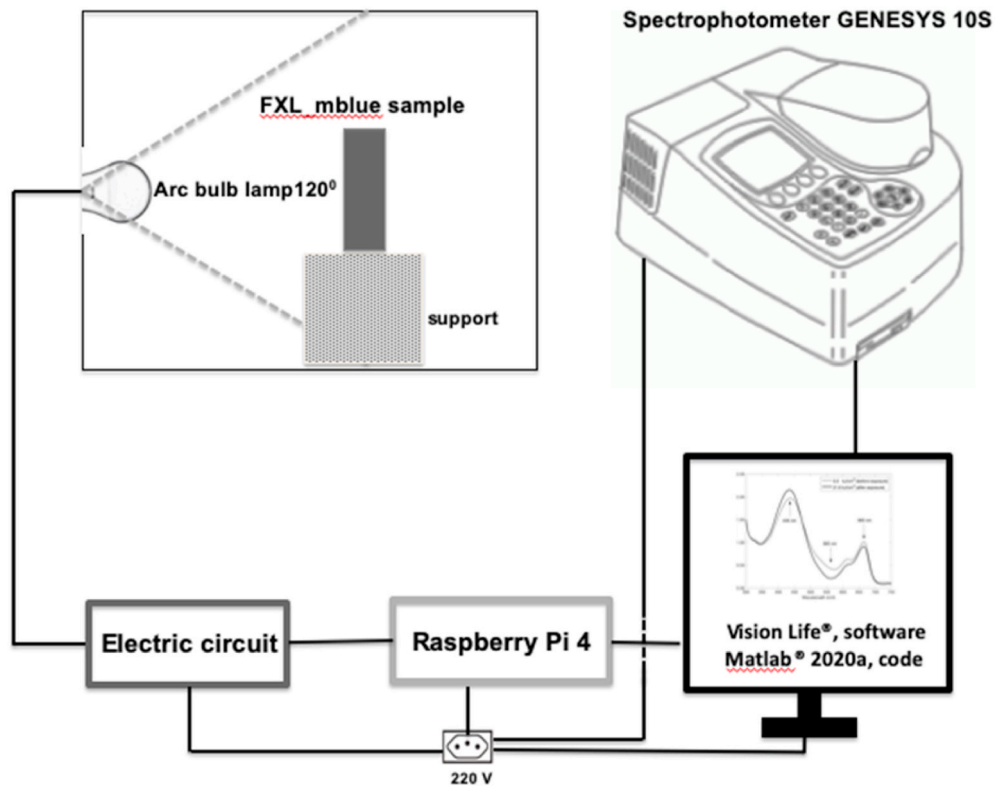


Fig. 1. Scheme of the experimental apparatus for the irradiations and evaluations of the samples of FXL-mblue.

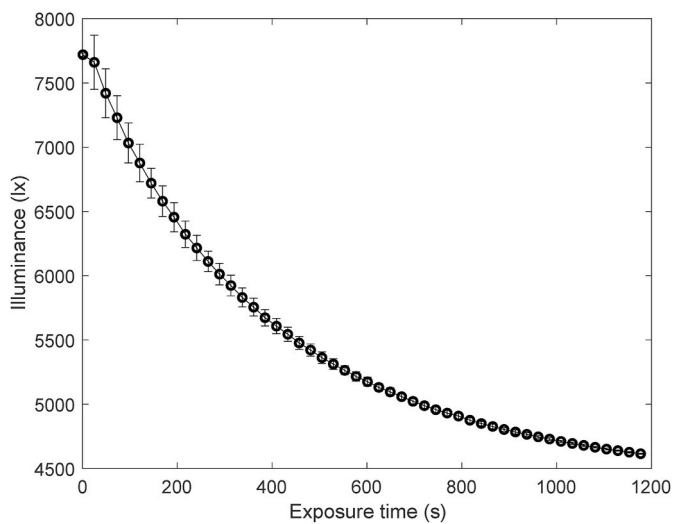


Fig. 2. Illuminance versus exposure time, for the red light source. The standard deviations are between 0.03% and 8.3%, corresponding to the minimum and maximum illuminance measurements, respectively.



Fig. 3. FXL-mblue samples: on the left side non-irradiated sample (0.00 kJ/cm²) and on the right side irradiated sample (21.6 kJ/cm²).

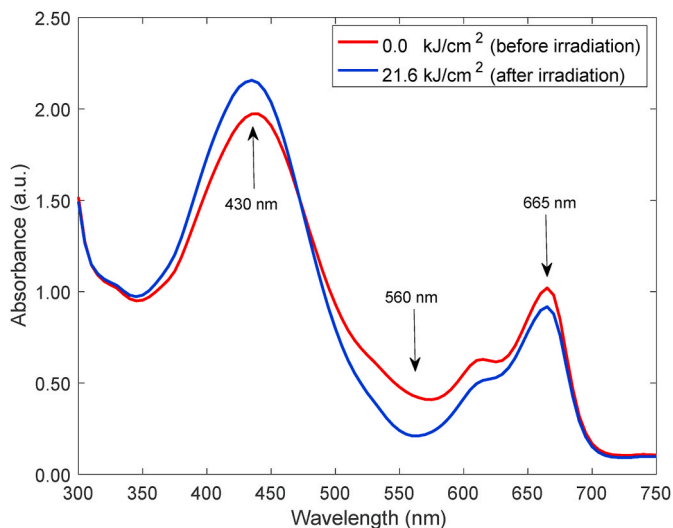


Fig. 4. UV-Vis spectra, absorbance versus wavelength, for FXL-mblue samples non-irradiated (0.0 kJ/cm^2) and irradiated (21.6 kJ/cm^2). In this case, the non-irradiated cuvette contained air.

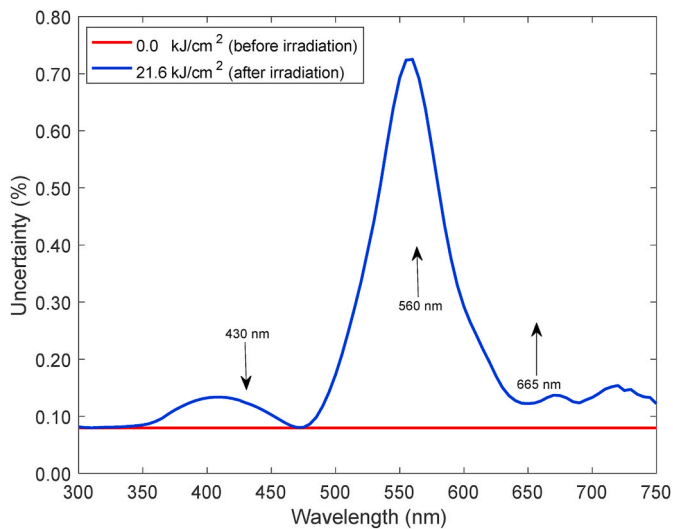


Fig. 5. Uncertainty versus wavelength, for FXL-mblue samples non-irradiated (0.0 kJ/cm^2) and irradiated (21.6 kJ/cm^2).

2. Materials and methods

2.1. Materials and equipment

The materials and equipment used in this work were: 1) Standard cuvettes with dimensions of $1 \times 1 \times 4.5 \text{ cm}^3$; 2) FXL solution prepared with the following reagents: i) xylene orange; ii) ferrous ammonium sulfate; iii) sulfuric acid and iv) methylene blue; all concentrations and other characteristics of the reagents are shown in Table 1; 3) Electrical circuit containing a 5 V–10 A (Songle®) relay with 1 channel; 4) Raspberry Computer Model B Pi 4 with 4 GB of RAM, quad-core Cortex-A72 processor clocked at 1.5 GHz; 5) The Genesys 10S/Thermo Scientific spectrophotometer with a carousel for 6 cuvettes; 6) A Macbook® pro computer with 8GB of RAM and 512GB of SSD; 7) An arc bulb lamp with 7 W of power and 620–750 nm wavelength from a red LED lamp (Par20/Iluutron LED Technology®, Guararema-SP, Brazil) with dimensions of 90 mm height x 64 mm diameter, 25 kh lifetime, opening angle 120° , E27 base, and it is free from heat and also from UV and IR radiation emissions.

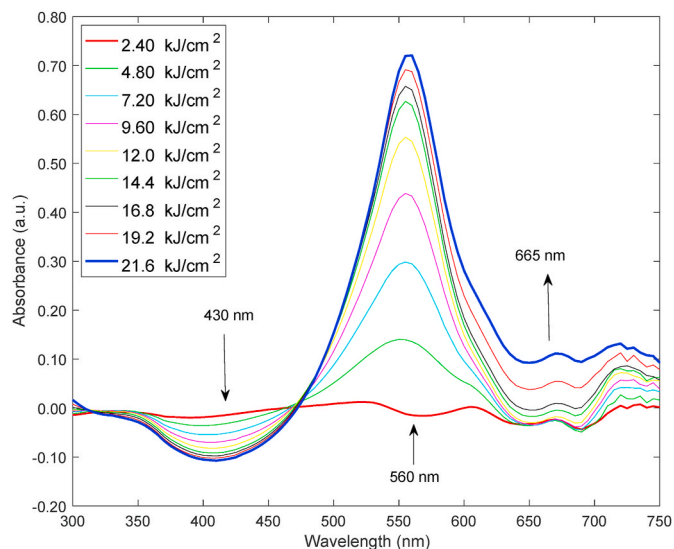


Fig. 6. Absorbance versus wavelength, for FXL-mblue samples for nine doses: 2.40 kJ/cm^2 , 4.80 kJ/cm^2 , 7.20 kJ/cm^2 , 9.60 kJ/cm^2 , 12.0 kJ/cm^2 , 14.4 kJ/cm^2 , 16.8 kJ/cm^2 , 19.2 kJ/cm^2 , and 21.6 kJ/cm^2 (red LED source). In this case, the non-irradiated cuvette contained FXL-mblue solution.

2.2. FXL-mblue detector preparation

The Fricke Xylenol Liquid (FXL-mblue) solution doped with methylene blue was obtained with the addition of 50% Milli-Q water in a beaker and adding xylene orange; immediately after, the sulfuric acid was added, and it was noticed that the color of the solution changed from purple to light orange. The remaining 50% of Milli-Q water was for the addition of ferrous sulfate and methylene blue, thus obtaining the final solution in a dark green color and inserted into cuvettes.

2.3. Apparatus for irradiation source and UV-Vis measurements

The scheme of the experimental apparatus for irradiation and evaluation of cuvettes containing FXL-mblue is presented in Fig. 1. Each cuvette is housed in a support and next to the red LED lamp which is fixed on a horizontal surface, and the cuvette was positioned within the opening angle of the lamp; the shape of the beam is uniform; this lamp is connected to an electrical circuit and to the Raspberry PI 4 micro controller. To control the time the lamp is on, a Matlab® 2020a code is used which controls the Raspberry PI 4, turning the circuit off or on. After the irradiations, the evaluation of the irradiated and non-irradiated cuvettes was performed on the Spectrophotometer Genesys UV-Vis 10S, from 300 nm to 750 nm, with 5 nm spectral resolution, and visualized on a computer screen by the UV-Vis Vision Life® software. All equipment is connected at a potential difference of 220 V.

2.4. Irradiation of FXL-mblue detector

The irradiations of the FXL-mblue samples were done using the red LED lamp, and then they were evaluated after nine exposure times of 20, 40, 60, 80, 100, 120, 140, 160 and 180 min which doses correspond to 2.40 , 4.80 , 7.20 , 9.60 , 12.0 , 14.4 , 16.8 , 19.2 , and 21.6 kJ/cm^2 , respectively. The distance from the LED lamp to the FXL-mblue sample was of 0.5 cm. The uncertainty was of type C, which considers the square root of the square for uncertainties B and the square sum for uncertainties A. The uncertainty of the reading equipment is of type B, while the uncertainty of the measurements was performed through the standard triplicate deviation for each irradiated or pos-irradiated sample, designed as type A.

For the evaluation of the red LED source, measurements of its

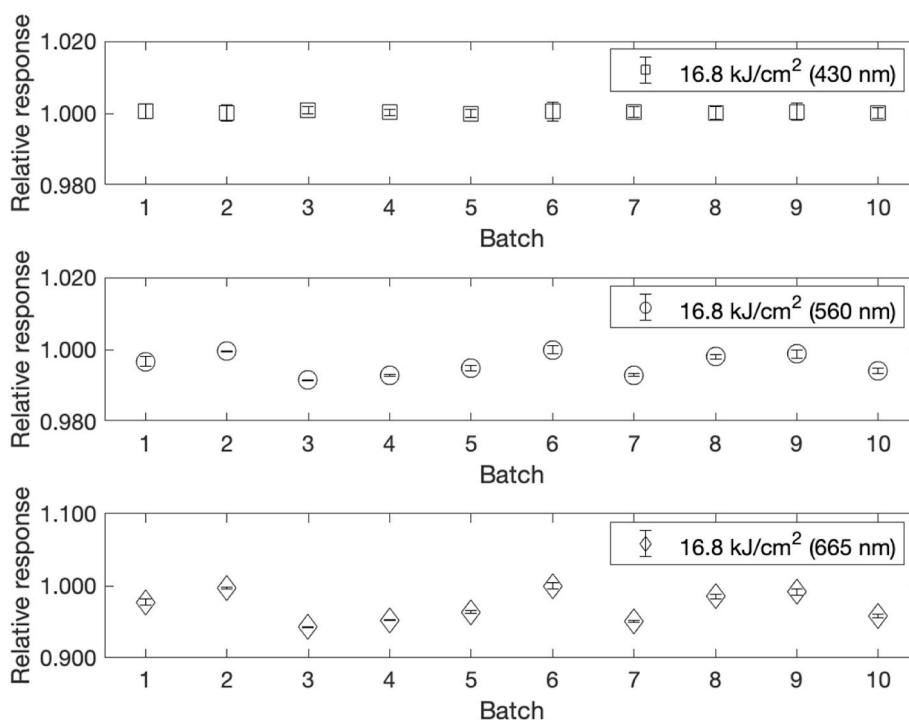


Fig. 7. Reproducibility of FXL-mblue detector irradiated with 16.8 kJ/cm² dose from red LED lamp, with wavelengths: a) 430 nm, b) 560 nm and c) 665 nm.

illuminance were associated with the exposure time. A luximeter (LDR-225/Instrutherm®) together with the Light Meter pro 8.0® software were utilized for the illuminance measurements. They were made under the same conditions of the irradiations.

2.5. General conditions for the investigation of FXL-mblue

The results were obtained from the application of the Law of Lambert Beer, which considers the negative of the logarithm of the ratio between the evaluated values of the irradiated and non-irradiated samples of FXL-mblue. After irradiation, the FXL-mblue samples were stored at room temperature and accommodated in a standard polystyrene box for cuvettes. All effects such as natural oxidation and also those associated with the heat incident on the samples were measured using UV-Vis spectroscopy up to six days after irradiation.

From the absorbance values it was possible to investigate: i) the spectrum of FXL-mblue with nine doses; ii) the uncertainties of the measurements; iii) linearity is then evaluated considering Pearson's correlation coefficient through the dose-response curve for all doses and also for the first five doses; iv) the sensitivity for all analyzed wavelengths; v) reproducibility of ten detector groups containing three samples in each group, the absolute value divided by the average absorbance value was determined as relative absorbance; vi) repeatability for FXL-mblue; vii) the minimum detectable dose (MDD) was also evaluated by multiplying the standard deviation by the factor three and divided by the sensitivity in the linear region; and viii) the fading of the signal with time.

3. Results and discussion

Fig. 2 shows the illuminance measurements *versus* exposure time, for the red LED light source. These data are in agreement with results of the literature [22], and a polynomial fit ($R^2 = 0.997$) was obtained. From this result, it was possible to infer the necessary time for the stability of the radiation system before the irradiations of FXL-mblue samples could start. This minimum time interval was determined as 20 min. From Fig. 2, the illuminance stability of the lamp occurs in 20 min, that is,

with the dose of 2.40 kJ/cm². In other words, it was chosen due to this minimum time of stability of the system; clearly after this stabilization time it is possible to have doses with values lower than 2.40 kJ/cm² and greater than 21.6 kJ/cm². In the case of the last dose (21.6 kJ/cm²), it was chosen due to the wavelengths 430 nm and 565 nm, which reached the saturation values for the their absorbances; for 665 nm this value was obtained in order to be irradiated with the doses that are used in photodynamic therapy.

Fig. 3 shows the samples of FXL-mblue irradiated and non-irradiated with the red LED source. From this result, the color change in the sample of the FXL-mblue detector can be inferred that it is a Yes/No irradiated detector for the dose interval analyzed in this work.

UV-Vis spectra for FXL-mblue sample before and after irradiation using the red LED lamp are presented in Fig. 4. In this figure, it is possible to identify 3 maximum peaks of absorbance, 430 nm, 560 nm and 665 nm. The first two peaks are commonly found in the Fricke Xylenol Gel (FXG) dosimeter solution, in which 430 nm and 560 nm represent the Fe²⁺ ions and the Fe³⁺-XO complex, respectively. One of the innovations of this work is the appearance of the third peak, at 665 nm, which is due to the methylene blue spectrum and has a maximum peak at the mentioned wavelength. It is also possible to observe that there is a difference in the absorbance values for samples before and after irradiation, thus indicating the possibility of application in the quality control program in photodynamic therapy. Statistically for the group of doses, $p < 0.01$ was considered significant.

Fig. 5 shows the uncertainty associated with wavenumber, for the FXL-mblue samples. The results of the uncertainties for the non-irradiated cuvettes were constant throughout the wavelength interval, obtaining the value of 0.08%. For the absorbance peaks at 430 nm, 560 nm and 665 nm, the uncertainty values were 0.12%, 0.72% and 0.13%, respectively. Thus, the maximum uncertainty was less than 1% for all samples for both non-irradiated samples and for the sample irradiated with the highest dose.

Results on UV-Vis spectra for FXL-mblue samples, absorbance *versus* wavelength, with doses from 2.40 kJ/cm² to 21.6 kJ/cm² (red LED source) are shown in Fig. 6. After irradiation of the FXL-mblue samples, three characteristic peaks were established, at wavelengths of 430 nm,

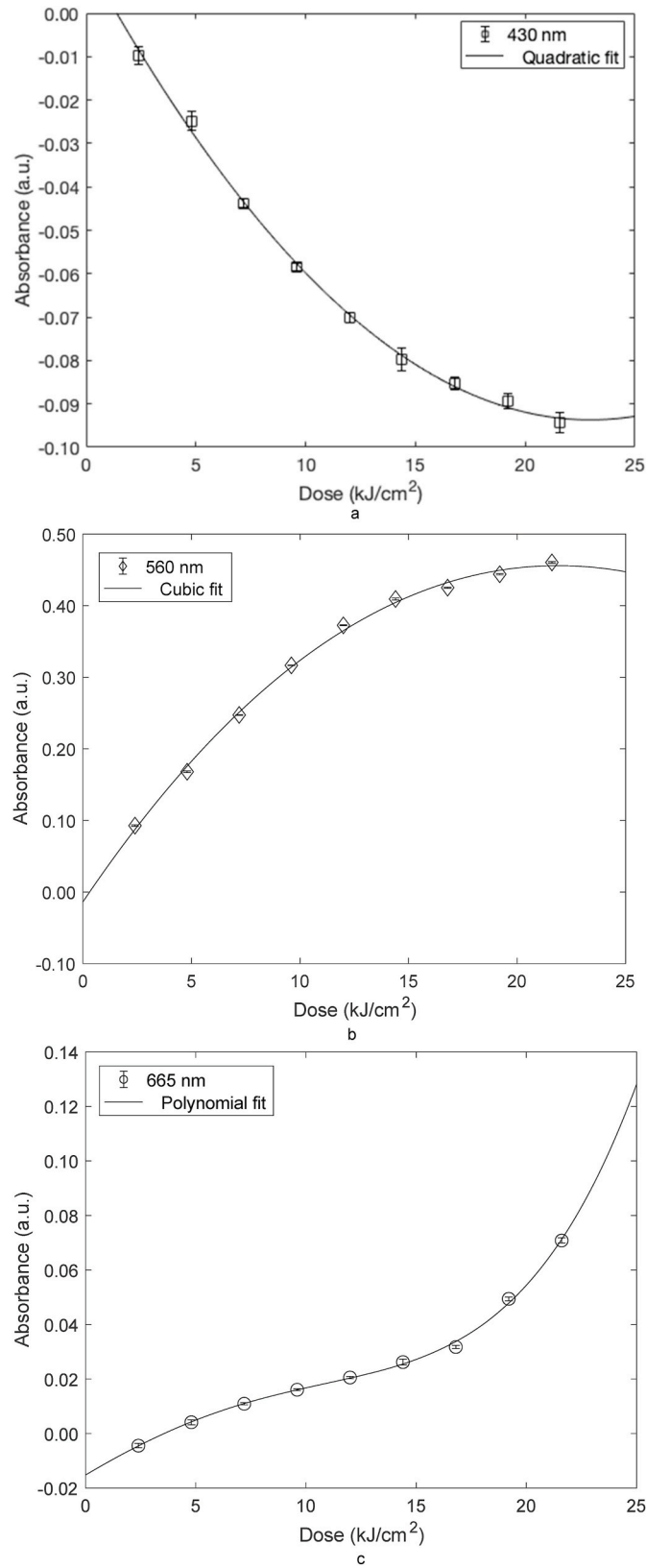


Fig. 8. Dose response curves for FXL-mblue detector irradiated with nine doses from red LED lamp, with wavelengths: a) 430 nm, b) 560 nm and c) 665 nm.

Table 2

Quadratic, cubic and polynomial fit equations and linear fit for five doses and nine doses, respectively. The respective linearities corresponding to the absorbance peaks at 430 nm, 560 nm and 665 nm are observed in the table. The values of y and x are the absorbance and doses respectively.

Wavelength (nm)	Equation (Fig. 7a, b and 7c)	Fit	R ²	Equation (Fig. 8a, b and 8c)	Fit	R ²
430	$y = 2.0e^{-4}x^2 - 0.009x + 0.012$	Quadratic	0.9982	$y = -6.4e^{-3}x + 0.005$	Linear	0.9936
560	$y = 8.7e^{-6}x^3 - 2.3e^{-3}x^2 + 0.090x - 0.227$	Cubic	0.9979	$y = 5.9e^{-2}x - 0.146$	Linear	0.9953
665	$y = 1.8e^{-6}x^4 - 3.4e^{-5}x^3 - 2.3e^{-4}x^2 - 0.012x - 0.038$	Polynomial	0.9984	$y = 6.4e^{-3}x - 0.023$	Linear	0.9822

560 nm and 665 nm. This last peak is new for detectors that present xylenol orange and ferrous sulfate in their solutions, such as Fricke Xylenol Gel (FXG); this addition of methylene blue provides another region that can be explored and researched for its linearity and irradiation sources such as the red LED lamp applied in this work. The methylene blue applied to the Fricke Xylenol Liquid (FXL) solution showed three very interesting characteristics: i) the color change from dark green to increasingly lighter green with the dose; ii) absorption peak at 665 nm, indicating the possibility of linear regions close to this peak; iii) as it is a photosensitizer, it was essential for the FXL solution to create sensitivity to light from the red LED. Both in these peaks and in nearby regions it can be inferred that the dose can be mathematically related to the absorbance for this detector.

Fig. 7 presents the reproducibility (relative response) as a function of the quantity of sample batches of the FXL-mblue detector to a 16.8 kJ/cm² dose and for 430 nm, 560 nm and 665 nm wavelengths. The average standard deviations for the ten batches of FXL-mblue with the wavelengths of 430 nm, 560 nm and 665 nm were $\pm 0.17\%$, $\pm 0.35\%$ and $\pm 0.42\%$. These values show that the detector in all analyzed wavelengths, and especially in the new wavelength (665 nm), can be easily reproduced. The response repeatability obtained for the wavelengths of 430 nm, 560 nm and 665 nm was $\pm 0.03\%$, $\pm 0.07\%$ and $\pm 0.23\%$, respectively. As the repeatability also provided good results, all below 1%, the new detector is easily reproducible as described in this work.

Fig. 8a, b and 8c show the absorbance versus dose, for 430 nm, 560 nm and 665 nm, respectively. The curve shape established between all nine doses and absorbance was determined by adjusting each curve with its respective wavelengths. The mathematical equations that describe each curve and with their best R² adjustments can be seen in Table 2; it shows the mathematical equations for the peak wavelengths and the R² ratio both for all doses and for a selection of five doses. It is possible to see that the absorbance values associated with the doses for the wavelength at 560 nm is greater than for the wavelengths of 665 nm and 430 nm.

For all doses it is possible to see that there is a tendency to saturation of the response with a maximum detectable dose for each wavelength; this happens from the fifth dose, that is 12.0 kJ/cm², for the wavelengths of 430 nm, 560 nm and 665 nm. This fact is associated with the conversion of iron ions in the solution and the sensitivity of the photosensitizer in the case of the last wavelength. Even for the 665 nm wavelength, it was possible to infer that there is a supralinear region with increasing doses. The minimum detectable dose (MDD) was also obtained: 0.610 ± 0.004 kJ/cm², 0.160 ± 0.003 kJ/cm², 0.510 ± 0.007 kJ/cm² for 430 nm, 560 nm and 665 nm, respectively. These maximum and minimum values are important because they define which dose values may be evaluated for the new detector.

Results about dose-response curves for 430 nm, 560 nm and 665 nm wavelengths are shown in Fig. 9a, b and 9c, respectively. These curves were evaluated for the first five doses, and the linear and R² adjustments can be seen in Table 2. The behavior of the curves are linear with R² equal to 0.9936, 0.9953 and 0.9822 for the wavelengths of 430 nm, 560 nm and 665 nm, respectively. These results demonstrate the effectiveness of the application of the new FXL-mblue detector in measurements with light beams from the red LED source. Table 3 shows results from the five and nine doses for FXL-mblue samples. As can be seen, there is a high number of wavelengths which show good linearity results; this

investigation confirms that not only the peaks provide good results for linearity. Statistically, the values of R², such as the standard deviation reaching close to zero and the dispersion of the data, can be considered adequate and uniform in the studied two cases, that is, there was no significantly dispersed point.

Absorbance sensitivity from the dose-response curves for five and nine values of doses versus wavelength are shown in Fig. 10. For the wavelengths which have the three peaks, 430 nm, 560 nm and 665 nm, the values of the sensitivity for five and nine doses are -0.0067 , 0.0596 , 0.0002 and -0.0046 , 0.0381 , 0.0055 , respectively. The sensitivities increased with a greater number of doses for the wavelengths of 430 nm and 665 nm; for the 560 nm wavelength it did not occur.

In Table 4 are presented the fading absorbance dates for six days storage at room-temperature. From these results it is possible to show that for non-irradiated samples (0.0 kJ/cm²) the values increase each day. For the irradiated samples (21.6 kJ/cm²) the opposite occurs, the values of the slopes for each day decrease. In other words, FXL-mblue can be considered stable over time, making the necessary corrections of absorbance over time, and it may be used even after a few days of its irradiation, considering the wavelength evaluated (430 nm, 560 nm or 665 nm). A better visualization of the fading results can be seen in Fig. 11a and b. The curves for 430 nm and 665 nm confirm the possibility of controlling the natural oxidation in the pre- and post-irradiation samples, that is, the stability of the detector.

4. Conclusions

For the samples of FXL-mblue, as a preliminary study, the following final aspects were observed: i) UV-Vis spectrophotometry is an adequate technique because in addition to quantitatively determining the exchanges of FXL-mblue placements, it is considered a low cost and non-destructive technique; it may be used in measurements of irradiated FXL-mblue samples; ii) the uncertainties arising from the absorbances of non-irradiated samples were less than 0.10% and for the highest dose with the longest wavelength the value was less than 0.80%; the presented results have a high reliability and repeatability; iii) all linearity results were satisfactorily evaluated for both nine and five doses, but regardless of the amount of doses, the dose-response curves could be mathematically adjusted, whether linear, cubic, quadratic or polynomial, thus showing that all the studied regions can be applied; iv) one of the most important results of this research was the sensitivity of FXL-mblue in the wavelength, the photosensitizer was stimulated in the methylene blue region at 665 nm causing its sensitivity to increase with the dose. In other regions the same impact occurred mainly on the 430 nm and 560 nm wavelength regions; v) from the results of the minimum detectable dose (MDD) it was possible to conclude that to make a simulation in photodynamic therapy the time spent would be around 80 s for a unique dose. In other words, the quality control using the irradiator system proposed in this work, together with the new detector, could easily be implemented in a photodynamic therapy service; vi) reproducibility and repeatability less than 1% somehow demonstrate the uniformity of the FXL-mblue solution with both the solution and the dose; vii) from the results of the response fading it can be concluded that they are small values and both the irradiated and non-irradiated samples tend to a balance; that is to say the values of the non-irradiated samples increase and the irradiated ones decrease, in a way the temporal

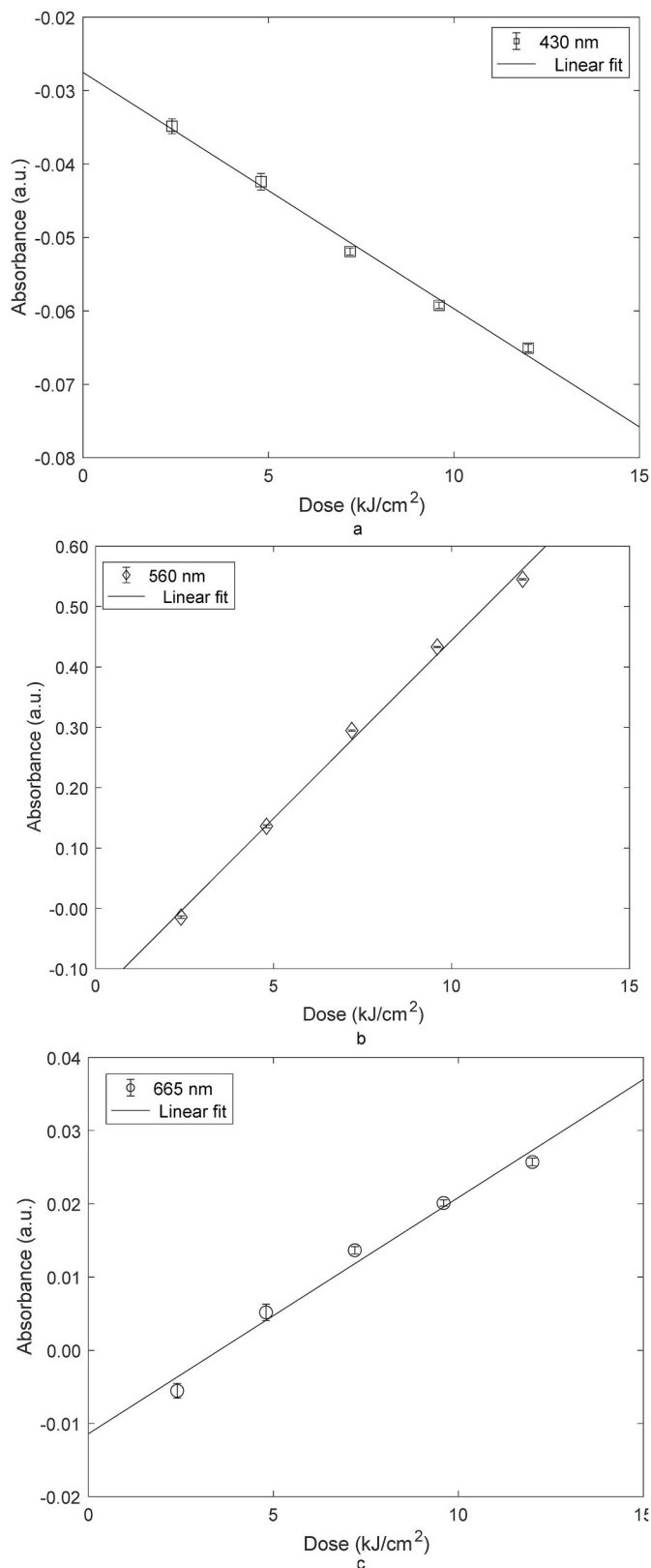


Fig. 9. Dose response curves for FXL-mblue detector irradiated with five doses from LED red lamp, with wavelengths: a) 430 nm, b) 560 nm and c) 665 nm.

corrections can be made through the obtained graphs. The advantages of the FXL-mblue samples compared to other dosimeters are: 1) Low cost reader technique in comparison with other techniques as for example Nuclear Magnetic Resonance (NMR) and Fourier Transform Infrared

(FTIR) spectroscopy; 2) They can be used both in radiotherapy and light bulb dosimetric measurements; 3) They do not need pre-processing; after irradiation, the detector may be evaluated immediately; 4) Dosimeter YES/NO and 5) As a liquid dosimeter, it can be inserted in a

Table 3

The summary of the linearity data for corresponding wavelength, to five doses (2.40–12.0 kJ/cm²) and nine doses (2.40–21.6 kJ/cm²).

Linearity (R ²) 2.40 up to 12.0 kJ/cm ²	Wavelength (nm)	Standard deviation	Coefficient of variation (%)	Linearity (R ²) 2.40 up to 21.6 kJ/cm ²	Wavelength (nm)	Standard deviation	Coefficient of variation (%)
0.9980	635	0.0625	0.0039	0.9964	365	0.0575	0.0033
0.9968	370	0.0624	0.0039	0.9936	370	0.0573	0.0032
0.9960	715	0.0623	0.0038	0.9852	465	0.0564	0.0031
0.9953	560	0.0623	0.0038	0.9825	740	0.0562	0.0031
0.9952	555	0.0623	0.0039	0.9784	375	0.0558	0.0031
0.9949	375	0.0622	0.0039	0.9779	735	0.0557	0.0031
0.9946	565	0.0622	0.0039	0.9767	470	0.0556	0.0030
0.9944	550	0.0622	0.0039	0.9766	725	0.0556	0.0030
0.9936	570	0.0621	0.0039	0.9746	720	0.0554	0.0030
0.9931	545	0.0621	0.0038	0.9715	460	0.0551	0.0030
0.9929	380	0.0621	0.0038	0.9706	605	0.0550	0.0030
0.9918	385	0.0620	0.0038	0.9705	360	0.0550	0.0030
0.9917	420	0.0620	0.0038	0.9702	715	0.0549	0.0030
0.9916	540	0.0620	0.0038	0.9684	600	0.0548	0.0030
0.9915	445	0.0619	0.0038	0.9659	730	0.0545	0.0029
0.9915	425	0.0619	0.0038	0.9646	380	0.0544	0.0029
0.9914	435	0.0619	0.0038	0.9635	610	0.0543	0.0029
0.9914	575	0.0619	0.0038	0.9633	310	0.0542	0.0029
0.9913	410	0.0619	0.0038	0.9580	745	0.0537	0.0028

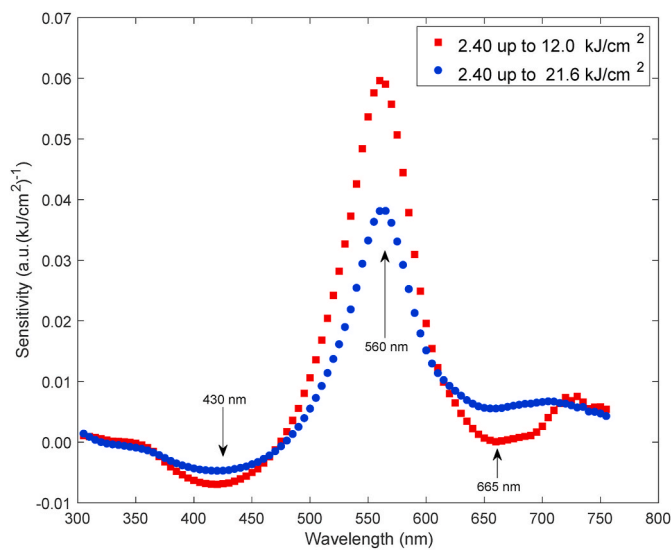


Fig. 10. Sensitivity versus wavelength of FXL-mblue samples for the doses 21.6 kJ/cm² and 0.0 kJ/cm².

Table 4

Slope absorbance versus day for doses 21.6 kJ/cm² and 0.0 kJ/cm², std is the standard deviation for the results of each column.

Day	21.6 kJ/cm ²			0.0 kJ/cm ²		
	430 nm std (±0.0093)	560 nm std (±0.0805)	665 nm std (±0.0049)	430 nm std (±0.2617)	560 nm std (±0.0839)	665 nm std (±0.0633)
1	-0.1055	0.7292	0.0847	2.0106	0.5510	0.6779
2	-0.1001	0.6862	0.0821	2.1175	0.5906	0.7117
3	-0.0951	0.6431	0.0794	2.2243	0.6302	0.7456
4	-0.0901	0.6001	0.0768	2.3312	0.6697	0.7794
5	-0.0850	0.5571	0.0742	2.4380	0.7093	0.8133
6	-0.0800	0.5140	0.0715	2.5448	0.7488	0.8471

container to obtain 3D dosimetry. In conclusion, the results of FXL-mblue samples indicate an acceptable linear response in function of dose, and therefore this material presents a potential use as a light radiation detector and for applications of quality control in photodynamic therapy.

CRedit author statement

Lucas Nonato de Oliveira: Conceptualization, Methodology, Validation, Formal analysis, Resources, Data Curation, Investigation, Resources, Writing - Original Draft, Writing - Review & Editing, Visualization, Funding acquisition. Eriberto Oliveira do Nascimento: Conceptualization, Validation Methodology, Software, Formal analysis, Data Curation, Writing - Review & Editing. Linda V.E. Caldas: Methodology, Supervision, Writing - Review & Editing, Funding acquisition.

Declaration of competing interest

The authors declare that they have no known competing financial interests or personal relationships that could have appeared to influence the work reported in this paper.

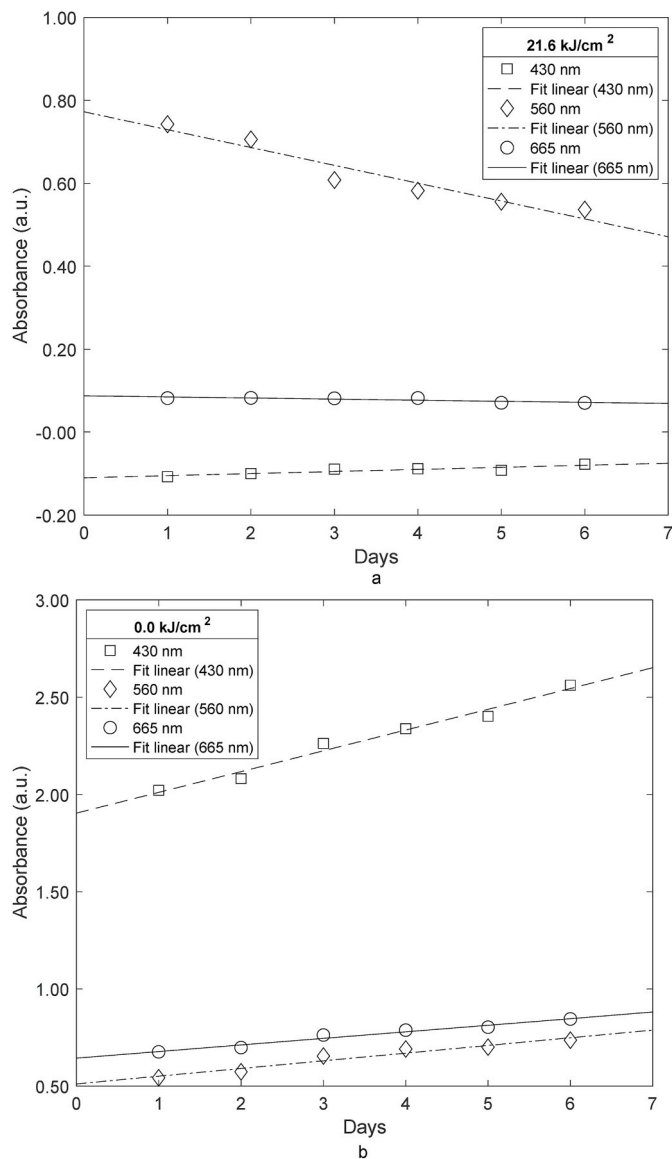


Fig. 11. Fading of FXL-mblue samples, room-temperature, in the 430 nm, 560 nm and 665 nm for doses: a) 21.6 kJ/cm² and b) 0.0 kJ/cm².

Acknowledgements

The authors thank the Brazilian funding agencies CNPq (Projects 104486/2019-8, and 301335/2016-8) and FAPESP (Project 2018/05982-0) for partial financial support. This paper is dedicated to the memory of Professor Robert Lee Zimmerman.

References

[1] A. Marini, L. Lazzeri, M.G. Cascone, R. Ciolini, L. Tana, F. d'Errico, Fricke gel dosimeters with low-diffusion and high-sensitivity based on a chemically cross-linked PVA matrix, *Radiat. Meas.* 106 (2017) 618–621, <https://doi.org/10.1016/j.radmeas.2017.02.012>.

[2] L. Pirani, L. de Oliveira, P. Petchevist, M. Moreira, D. Ila, A. de Almeida, New chemical Fricke gel radiation dosimeter, *J. Radioanal. Nucl. Chem.* 280 (2009) 259–264, <https://doi.org/10.1007/s10967-009-0508-6>.

[3] T. Maeyama, N. Fukunishi, K.L. Ishikawa, K. Fukasaku, S. Fukuda, Radiological properties of nanocomposite Fricke gel dosimeters for heavy ion beams, *J. Radiat. Res.* 57 (2016) 318–324, <https://doi.org/10.1093/jrr/rrw025>.

[4] M.S. Alva-Sánchez, L.N. de Oliveira, P.C. Petchevist, M.V. Moreira, A. de Almeida, Beta planar source quality assurance with the Fricke xylene gel dosimeter, *Radiat. Phys. Chem.* 96 (2014) 56–59, accessed May 4, 2020, <https://www.sciencedirect.com/science/article/abs/pii/S0969806X13004994>.

[5] H. Fricke, S. Morse, The chemical action of roentgen rays on dilute ferrousulphate solutions as a measure of dose, *Am. J. Roentgenol. Radium Ther. Nucl. Med.* 18 (1927) 430–432.

[6] M.A. Bero, W.B. Gilboy, P.M. Glover, H.M. El-Masri, Tissue-equivalent gel for non-invasive spatial radiation dose measurements, *Nucl. Instrum. Methods Phys. Res. Sect. B Beam Interact. Mater. Atoms* 166 (2000) 820–825.

[7] J.B. Davies, C. Baldock, Temperature dependence on the dose response of the Fricke-gelatin-xylene orange gel dosimeter, *Radiat. Phys. Chem.* 79 (2010) 660–662, <https://doi.org/10.1016/j.radphyschem.2009.11.014>.

[8] R.G. Kelly, K.J. Jordan, J.J. Battista, Optical CT reconstruction of 3D dose distributions using the ferrous-benzoic-xylene (FBX) gel dosimeter, *Med. Phys.* 25 (1998) 1741–1750.

[9] M.A. Bero, W.B. Gilboy, P.M. Glover, J.L. Keddie, Three-dimensional radiation dose measurements with ferrous benzoic acid xylene orange in gelatin gel and optical absorption tomography, *Nucl. Instrum. Methods Phys. Res. Sect. A Accel. Spectrom. Detect. Assoc. Equip.* 422 (1999) 617–620.

[10] J. Vedelago, F. Mattea, M. Valente, Integration of Fricke gel dosimetry with Ag nanoparticles for experimental dose enhancement determination in theranostics, *Appl. Radiat. Isot.* 141 (2018) 182–186, <https://doi.org/10.1016/j.apradiso.2018.02.028>.

[11] G. Collura, S. Gallo, L. Tranchina, B.F. Abbate, A. Bartolotta, F. d'Errico, M. Marrale, Analysis of the response of PVA-GTA Fricke-gel dosimeters with clinical magnetic resonance imaging, *Nucl. Instrum. Methods Phys. Res. Sect. B Beam Interact. Mater. Atoms* 414 (2018) 146–153, <https://doi.org/10.1016/j.nimb.2017.06.012>.

[12] W. Parwaie, G. Geraily, A. Shirazi, A. Shakeri, H. Massumi, M. Farzin, Analysis of the ferrous benzoic methylthymol-blue gel dosimeter in low-dose-level measurements, *Radiat. Phys. Chem.* 173 (2020) 108943, <https://doi.org/10.1016/j.radphyschem.2020.108943>.

[13] K.A. Rabaeh, T.F. Hailat, M.M. Eyadeh, M.Y. Al-Shorman, F.M. Aldweri, S. M. Alheet, B.G. Madas, S.I. Awad, Dosimetric properties of sulfosalicylic acid-ferrous-polyvinyl alcohol-glutaraldehyde hydrogel dosimeters using magnetic and optical techniques, *Radiat. Phys. Chem.* 177 (2020) 109106, <https://doi.org/10.1016/j.radphyschem.2020.109106>.

[14] S. Lazzaroni, G.M. Liosi, M. Mariani, D. Dondi, An innovative Fe³⁺ selective ligand for Fricke-gel dosimeter, *Radiat. Phys. Chem.* 171 (2020) 108733, <https://doi.org/10.1016/j.radphyschem.2020.108733>.

[15] J.B. Davies, C. Baldock, Sensitivity and stability of the Fricke-gelatin-xylene orange gel dosimeter, *Radiat. Phys. Chem.* 77 (2008) 690–696.

[16] C. Guzman Calcina, N. de Oliveira, C. de Almeida, A. Almeida, Dosimetric parameters for small field sizes using Fricke xylene gel, thermoluminescent and film dosimeters, and an ionization chamber, *Phys. Med. Biol.* 52 (2007) 1431–1439, <https://doi.org/10.1088/0031-9155/52/5/014>.

[17] Y. Soliman, M. Abdelgawad, Fricke gel dosimeter as a tool in quality assurance of the radiotherapy treatment plans, *Appl. Radiat. Isot.* 120 (2017), <https://doi.org/10.1016/j.apradiso.2016.12.004>.

[18] C. Xie, H. Zhu, S. Chen, Y. Wen, L. Jin, L. Zhang, J. Tong, Y. Shen, Chronic retinal injury induced by white LED light with different correlated color temperatures as determined by microarray analyses of genome-wide expression patterns in mice, *J. Photochem. Photobiol. B Biol.* 210 (2020) 111977, <https://doi.org/10.1016/j.jphotobiol.2020.111977>.

[19] I. Abukassem, M. Bero, Application of radiochromic gel detector (FXG) for UVA dose measurements, *Radiat. Phys. Chem.* 79 (2010) 1209, <https://doi.org/10.1016/j.radphyschem.2010.06.010>.

[20] S. Santos, V. Souza, Fricke dosimetry as a tool to quality control of photodynamic therapy, *Brazilian Journal of Radiation Sciences* 7 (2019), <https://doi.org/10.15392/bjrs.v7i3.427>.

[21] P. Agostinis, K. Berg, K.A. Cengel, T.H. Foster, A.W. Girotti, S.O. Gollnick, S. M. Hahn, M.R. Hamblin, A. Juzeniene, D. Kessel, M. Korbelik, J. Moan, P. Mroz, D. Nowis, J. Piette, B.C. Wilson, J. Golab, Photodynamic therapy of cancer: an update, *CA, A Cancer Journal for Clinicians* 61 (2011) 250–281, <https://doi.org/10.3322/caac.20114>.

[22] V.S. Popov, E.I. Rummyantseva, H. Cengiz, Light meter CEM DT-1309 data acquisition with LabVIEW, in: 2015 International Siberian Conference on Control and Communications, SIBCON, 2015, pp. 1–4.